

Observation of the $\psi(1^3D_2)$ state in $e^+e^- \rightarrow \pi^+\pi^-\gamma\chi_{c1}$ at BESIII

M. Ablikim¹, M. N. Achasov^{9,a}, X. C. Ai¹, O. Albayrak⁵, M. Albrecht⁴, D. J. Ambrose⁴⁴, A. Amoroso^{48A,48C}, F. F. An¹, Q. An⁴⁵, J. Z. Bai¹, R. Baldini Ferroli^{20A}, Y. Ban³¹, D. W. Bennett¹⁹, J. V. Bennett⁵, M. Bertani^{20A}, D. Bettoni^{21A}, J. M. Bian⁴³, F. Bianchi^{48A,48C}, E. Boger^{23,h}, O. Bondarenko²⁵, I. Boyko²³, R. A. Briere⁵, H. Cai⁵⁰, X. Cai¹, O. Cakir^{40A,b}, A. Calcaterra^{20A}, G. F. Cao¹, S. A. Cetin^{40B}, J. F. Chang¹, G. Chelkov^{23,c}, G. Chen¹, H. S. Chen¹, H. Y. Chen², J. C. Chen¹, M. L. Chen¹, S. J. Chen²⁹, X. Chen¹, X. R. Chen²⁶, Y. B. Chen¹, H. P. Cheng¹⁷, X. K. Chu³¹, G. Cibinetto^{21A}, D. Cronin-Hennessy⁴³, H. L. Dai¹, J. P. Dai³⁴, A. Dbeyssi¹⁴, D. Dedovich²³, Z. Y. Deng¹, A. Denig²², I. Denysenko²³, M. Destefanis^{48A,48C}, F. De Mori^{48A,48C}, Y. Ding²⁷, C. Dong³⁰, J. Dong¹, L. Y. Dong¹, M. Y. Dong¹, S. X. Du⁵², P. F. Duan¹, J. Z. Fan³⁹, J. Fang¹, S. S. Fang¹, X. Fang⁴⁵, Y. Fang¹, L. Fava^{48B,48C}, F. Feldbauer²², G. Felici^{20A}, C. Q. Feng⁴⁵, E. Fioravanti^{21A}, M. Fritsch^{14,22}, C. D. Fu¹, Q. Gao¹, Y. Gao³⁹, Z. Gao⁴⁵, I. Garzia^{21A}, C. Geng⁴⁵, K. Goetzen¹⁰, W. X. Gong¹, W. Gradl²², M. Greco^{48A,48C}, M. H. Gu¹, Y. T. Gu¹², Y. H. Guan¹, A. Q. Guo¹, L. B. Guo²⁸, Y. Guo¹, Y. P. Guo²², Z. Haddadi²⁵, A. Hafner²², S. Han⁵⁰, Y. L. Han¹, X. Q. Hao¹⁵, F. A. Harris⁴², K. L. He¹, Z. Y. He³⁰, T. Held⁴, Y. K. Heng¹, Z. L. Hou¹, C. Hu²⁸, H. M. Hu¹, J. F. Hu^{48A,48C}, T. Hu¹, Y. Hu¹, G. M. Huang⁶, G. S. Huang⁴⁵, H. P. Huang⁵⁰, J. S. Huang¹⁵, X. T. Huang³³, Y. Huang²⁹, T. Hussain⁴⁷, Q. Ji¹, Q. P. Ji³⁰, X. B. Ji¹, X. L. Ji¹, L. L. Jiang¹, L. W. Jiang⁵⁰, X. S. Jiang¹, J. B. Jiao³³, Z. Jiao¹⁷, D. P. Jin¹, S. Jin¹, T. Johansson⁴⁹, A. Julin⁴³, N. Kalantar-Nayestanaki²⁵, X. L. Kang¹, X. S. Kang³⁰, M. Kavatsyuk²⁵, B. C. Ke⁵, R. Kliemt¹⁴, B. Kloss²², O. B. Kolcu^{40B,d}, B. Kopf⁴, M. Kornicer⁴², W. Kuehn²⁴, A. Kupsc⁴⁹, W. Lai¹, J. S. Lange²⁴, M. Lara¹⁹, P. Larin¹⁴, C. Leng^{48C}, C. H. Li¹, Cheng Li⁴⁵, D. M. Li⁵², F. Li¹, G. Li¹, H. B. Li¹, J. C. Li¹, Jin Li³², K. Li¹³, K. Li³³, Lei Li³, P. R. Li⁴¹, T. Li³³, W. D. Li¹, W. G. Li¹, X. L. Li³³, X. M. Li¹², X. N. Li¹, X. Q. Li³⁰, Z. B. Li³⁸, H. Liang⁴⁵, Y. F. Liang³⁶, Y. T. Liang²⁴, G. R. Liao¹¹, D. X. Lin¹⁴, B. J. Liu¹, C. X. Liu¹, F. H. Liu³⁵, Fang Liu¹, Feng Liu⁶, H. B. Liu¹², H. H. Liu¹⁶, H. H. Liu¹, H. M. Liu¹, J. Liu¹, J. P. Liu⁵⁰, J. Y. Liu¹, K. Liu³⁹, K. Y. Liu²⁷, L. D. Liu³¹, P. L. Liu¹, Q. Liu⁴¹, S. B. Liu⁴⁵, X. Liu²⁶, X. X. Liu⁴¹, Y. B. Liu³⁰, Z. A. Liu¹, Zhiqiang Liu¹, Zhiqing Liu²², H. Loehner²⁵, X. C. Lou^{1,e}, H. J. Lu¹⁷, J. G. Lu¹, R. Q. Lu¹⁸, Y. Lu¹, Y. P. Lu¹, C. L. Luo²⁸, M. X. Luo⁵¹, T. Luo⁴², X. L. Luo¹, M. Lv¹, X. R. Lyu⁴¹, F. C. Ma²⁷, H. L. Ma¹, L. L. Ma³³, Q. M. Ma¹, S. Ma¹, T. Ma¹, X. N. Ma³⁰, X. Y. Ma¹, F. E. Maas¹⁴, M. Maggiora^{48A,48C}, Q. A. Malik⁴⁷, Y. J. Mao³¹, Z. P. Mao¹, S. Marcello^{48A,48C}, J. G. Messchendorp²⁵, J. Min¹, T. J. Min¹, R. E. Mitchell¹⁹, X. H. Mo¹, Y. J. Mo⁶, C. Morales Morales¹⁴, K. Moriya¹⁹, N. Yu. Muchnoi^{9,a}, H. Muramatsu⁴³, Y. Nefedov²³, F. Nerling¹⁴, I. B. Nikolaev^{9,a}, Z. Ning¹, S. Nisar⁸, S. L. Niu¹, X. Y. Niu¹, S. L. Olsen³², Q. Ouyang¹, S. Pacetti^{20B}, P. Patteri^{20A}, M. Pelizaeus⁴, H. P. Peng⁴⁵, K. Peters¹⁰, J. Pettersson⁴⁹, J. L. Ping²⁸, R. G. Ping¹, R. Poling⁴³, Y. N. Pu¹⁸, M. Qi²⁹, S. Qian¹, C. F. Qiao⁴¹, L. Q. Qin³³, N. Qin⁵⁰, X. S. Qin¹, Y. Qin³¹, Z. H. Qin¹, J. F. Qiu¹, K. H. Rashid⁴⁷, C. F. Redmer²², H. L. Ren¹⁸, M. Ripka²², G. Rong¹, X. D. Ruan¹², V. Santoro^{21A}, A. Sarantsev^{23,f}, M. Savrie^{21B}, K. Schoenning⁴⁹, S. Schumann²², W. Shan³¹, M. Shao⁴⁵, C. P. Shen², P. X. Shen³⁰, X. Y. Shen¹, H. Y. Sheng¹, W. M. Song¹, X. Y. Song¹, S. Sosio^{48A,48C}, S. Spataro^{48A,48C}, G. X. Sun¹, J. F. Sun¹⁵, S. S. Sun¹, Y. J. Sun⁴⁵, Y. Z. Sun¹, Z. J. Sun¹, Z. T. Sun¹⁹, C. J. Tang³⁶, X. Tang¹, I. Tapan^{40C}, E. H. Thorndike⁴⁴, M. Tiemens²⁵, D. Toth⁴³, M. Ullrich²⁴, I. Uman^{40B}, G. S. Varner⁴², B. Wang³⁰, B. L. Wang⁴¹, D. Wang³¹, D. Y. Wang³¹, K. Wang¹, L. L. Wang¹, L. S. Wang¹, M. Wang³³, P. Wang¹, P. L. Wang¹, Q. J. Wang¹, S. G. Wang³¹, W. Wang¹, X. F. Wang³⁹, Y. D. Wang^{20A}, Y. F. Wang¹, Y. Q. Wang²², Z. Wang¹, Z. G. Wang¹, Z. H. Wang⁴⁵, Z. Y. Wang¹, T. Weber²², D. H. Wei¹¹, J. B. Wei³¹, P. Weidenkaff²², S. P. Wen¹, U. Wiedner⁴, M. Wolke⁴⁹, L. H. Wu¹, Z. Wu¹, L. G. Xia³⁹, Y. Xia¹⁸, D. Xiao¹, Z. J. Xiao²⁸, Y. G. Xie¹, Q. L. Xiu¹, G. F. Xu¹, L. Xu¹, Q. J. Xu¹³, Q. N. Xu⁴¹, X. P. Xu³⁷, L. Yan⁴⁵, W. B. Yan⁴⁵, W. C. Yan⁴⁵, Y. H. Yan¹⁸, H. X. Yang¹, L. Yang⁵⁰, Y. Yang⁶, Y. X. Yang¹¹, H. Ye¹, M. Ye¹, M. H. Ye⁷, J. H. Yin¹, B. X. Yu¹, C. X. Yu³⁰, H. W. Yu³¹, J. S. Yu²⁶, C. Z. Yuan¹, W. L. Yuan²⁹, Y. Yuan¹, A. Yuncu^{40B,g}, A. A. Zafar⁴⁷, A. Zallo^{20A}, Y. Zeng¹⁸, B. X. Zhang¹, B. Y. Zhang¹, C. Zhang²⁹, C. C. Zhang¹, D. H. Zhang¹, H. H. Zhang³⁸, H. Y. Zhang¹, J. J. Zhang¹, J. L. Zhang¹, J. Q. Zhang¹, J. W. Zhang¹, J. Y. Zhang¹, J. Z. Zhang¹, K. Zhang¹, L. Zhang¹, S. H. Zhang¹, X. Y. Zhang³³, Y. Zhang¹, Y. H. Zhang¹, Y. T. Zhang⁴⁵, Z. H. Zhang⁶, Z. P. Zhang⁴⁵, Z. Y. Zhang⁵⁰, G. Zhao¹, J. W. Zhao¹, J. Y. Zhao¹, J. Z. Zhao¹, Lei Zhao⁴⁵, Ling Zhao¹, M. G. Zhao³⁰, Q. Zhao¹, Q. W. Zhao¹, S. J. Zhao⁵², T. C. Zhao¹, Y. B. Zhao¹, Z. G. Zhao⁴⁵, A. Zhemchugov^{23,h}, B. Zheng⁴⁶, J. P. Zheng¹, W. J. Zheng³³, Y. H. Zheng⁴¹, B. Zhong²⁸, L. Zhou¹, Li Zhou³⁰, X. Zhou⁵⁰, X. K. Zhou⁴⁵, X. R. Zhou⁴⁵, X. Y. Zhou¹, K. Zhu¹, K. J. Zhu¹, S. Zhu¹, X. L. Zhu³⁹, Y. C. Zhu⁴⁵, Y. S. Zhu¹, Z. A. Zhu¹, J. Zhuang¹, L. Zotti^{48A,48C}, B. S. Zou¹, J. H. Zou¹

(BESIII Collaboration)

¹ Institute of High Energy Physics, Beijing 100049, People's Republic of China

² Beihang University, Beijing 100191, People's Republic of China

³ Beijing Institute of Petrochemical Technology, Beijing 102617, People's Republic of China

⁴ Bochum Ruhr-University, D-44780 Bochum, Germany

⁵ Carnegie Mellon University, Pittsburgh, Pennsylvania 15213, USA

- ⁶ *Central China Normal University, Wuhan 430079, People's Republic of China*
- ⁷ *China Center of Advanced Science and Technology, Beijing 100190, People's Republic of China*
- ⁸ *COMSATS Institute of Information Technology, Lahore, Defence Road, Off Raiwind Road, 54000 Lahore, Pakistan*
- ⁹ *G.I. Budker Institute of Nuclear Physics SB RAS (BINP), Novosibirsk 630090, Russia*
- ¹⁰ *GSI Helmholtzcentre for Heavy Ion Research GmbH, D-64291 Darmstadt, Germany*
- ¹¹ *Guangxi Normal University, Guilin 541004, People's Republic of China*
- ¹² *GuangXi University, Nanning 530004, People's Republic of China*
- ¹³ *Hangzhou Normal University, Hangzhou 310036, People's Republic of China*
- ¹⁴ *Helmholtz Institute Mainz, Johann-Joachim-Becher-Weg 45, D-55099 Mainz, Germany*
- ¹⁵ *Henan Normal University, Xinxiang 453007, People's Republic of China*
- ¹⁶ *Henan University of Science and Technology, Luoyang 471003, People's Republic of China*
- ¹⁷ *Huangshan College, Huangshan 245000, People's Republic of China*
- ¹⁸ *Hunan University, Changsha 410082, People's Republic of China*
- ¹⁹ *Indiana University, Bloomington, Indiana 47405, USA*
- ²⁰ *(A)INFN Laboratori Nazionali di Frascati, I-00044, Frascati, Italy; (B)INFN and University of Perugia, I-06100, Perugia, Italy*
- ²¹ *(A)INFN Sezione di Ferrara, I-44122, Ferrara, Italy; (B)University of Ferrara, I-44122, Ferrara, Italy*
- ²² *Johannes Gutenberg University of Mainz, Johann-Joachim-Becher-Weg 45, D-55099 Mainz, Germany*
- ²³ *Joint Institute for Nuclear Research, 141980 Dubna, Moscow region, Russia*
- ²⁴ *Justus Liebig University Giessen, II. Physikalisches Institut, Heinrich-Buff-Ring 16, D-35392 Giessen, Germany*
- ²⁵ *KVI-CART, University of Groningen, NL-9747 AA Groningen, The Netherlands*
- ²⁶ *Lanzhou University, Lanzhou 730000, People's Republic of China*
- ²⁷ *Liaoning University, Shenyang 110036, People's Republic of China*
- ²⁸ *Nanjing Normal University, Nanjing 210023, People's Republic of China*
- ²⁹ *Nanjing University, Nanjing 210093, People's Republic of China*
- ³⁰ *Nankai University, Tianjin 300071, People's Republic of China*
- ³¹ *Peking University, Beijing 100871, People's Republic of China*
- ³² *Seoul National University, Seoul, 151-747 Korea*
- ³³ *Shandong University, Jinan 250100, People's Republic of China*
- ³⁴ *Shanghai Jiao Tong University, Shanghai 200240, People's Republic of China*
- ³⁵ *Shanxi University, Taiyuan 030006, People's Republic of China*
- ³⁶ *Sichuan University, Chengdu 610064, People's Republic of China*
- ³⁷ *Soochow University, Suzhou 215006, People's Republic of China*
- ³⁸ *Sun Yat-Sen University, Guangzhou 510275, People's Republic of China*
- ³⁹ *Tsinghua University, Beijing 100084, People's Republic of China*
- ⁴⁰ *(A)Istanbul Aydin University, 34295 Sefakoy, Istanbul, Turkey; (B)Dogus University, 34722 Istanbul, Turkey; (C)Uludag University, 16059 Bursa, Turkey*
- ⁴¹ *University of Chinese Academy of Sciences, Beijing 100049, People's Republic of China*
- ⁴² *University of Hawaii, Honolulu, Hawaii 96822, USA*
- ⁴³ *University of Minnesota, Minneapolis, Minnesota 55455, USA*
- ⁴⁴ *University of Rochester, Rochester, New York 14627, USA*
- ⁴⁵ *University of Science and Technology of China, Hefei 230026, People's Republic of China*
- ⁴⁶ *University of South China, Hengyang 421001, People's Republic of China*
- ⁴⁷ *University of the Punjab, Lahore-54590, Pakistan*
- ⁴⁸ *(A)University of Turin, I-10125, Turin, Italy; (B)University of Eastern Piedmont, I-15121, Alessandria, Italy; (C)INFN, I-10125, Turin, Italy*
- ⁴⁹ *Uppsala University, Box 516, SE-75120 Uppsala, Sweden*
- ⁵⁰ *Wuhan University, Wuhan 430072, People's Republic of China*
- ⁵¹ *Zhejiang University, Hangzhou 310027, People's Republic of China*
- ⁵² *Zhengzhou University, Zhengzhou 450001, People's Republic of China*
- ^a *Also at the Novosibirsk State University, Novosibirsk, 630090, Russia*
- ^b *Also at Ankara University, 06100 Tandogan, Ankara, Turkey*
- ^c *Also at the Moscow Institute of Physics and Technology, Moscow 141700, Russia and*

at the Functional Electronics Laboratory, Tomsk State University, Tomsk, 634050, Russia

^d Currently at Istanbul Arel University, 34295 Istanbul, Turkey

^e Also at University of Texas at Dallas, Richardson, Texas 75083, USA

^f Also at the NRC "Kurchatov Institute", PNPI, 188300, Gatchina, Russia

^g Also at Bogazici University, 34342 Istanbul, Turkey

^h Also at the Moscow Institute of Physics and Technology, Moscow 141700, Russia

(Dated: September 20, 2018)

We report the observation of the $X(3823)$ in the process $e^+e^- \rightarrow \pi^+\pi^-X(3823) \rightarrow \pi^+\pi^-\gamma\chi_{c1}$ with a statistical significance of 6.2σ , in data samples at center-of-mass energies $\sqrt{s}=4.230, 4.260, 4.360, 4.420$ and 4.600 GeV collected with the BESIII detector at the BEPCII electron positron collider. The measured mass of the $X(3823)$ is $(3821.7 \pm 1.3 \pm 0.7)$ MeV/ c^2 , where the first error is statistical and the second systematic, and the width is less than 16 MeV at the 90% confidence level. The products of the Born cross sections for $e^+e^- \rightarrow \pi^+\pi^-X(3823)$ and the branching ratio $\mathcal{B}[X(3823) \rightarrow \gamma\chi_{c1,c2}]$ are also measured. These measurements are in good agreement with the assignment of the $X(3823)$ as the $\psi(1^3D_2)$ charmonium state.

PACS numbers: 13.20.Gd, 13.25.Gv, 14.40.Pq

Since its discovery, charmonium - meson particles which contain a charm and an anti-charm quark - has been an excellent tool for probing Quantum Chromodynamics (QCD), the fundamental theory that describes the strong interactions between quarks and gluons, in the non-perturbative (low-energy, long-distance effects) regime, and remains of high interest both experimentally and theoretically. All of the charmonium states with masses that are below the open-charm threshold have been firmly established [1, 2]; open-charm refers to mesons containing a charm quark (antiquark) and either an up or down antiquark (quark), such as D or \bar{D} . However, the observation of the spectrum that are above the open-charm threshold remains unsettled. During the past decade, many new charmoniumlike states were discovered, such as the $X(3872)$ [3], the $Y(4260)$ [4, 5] and the $Z_c(3900)$ [5–7]. These states provide strong evidence for the existence of exotic hadron states [8]. Although charged charmoniumlike states like the $Z_c(3900)$ provide convincing evidence for the existence of multi-quark states [9], it is more difficult to distinguish neutral candidate exotic states from conventional charmonium. Moreover, the study of transitions between charmonium(like) states, such as the $Y(4260) \rightarrow \gamma X(3872)$ [10], is an important approach to probe their nature, and the connections between them. Thus, a more complete understanding of the charmonium(like) spectroscopy and their relations is necessary and timely.

The lightest charmonium state above the $D\bar{D}$ threshold is the $\psi(3770)$ [2], which is currently identified as the 1^3D_1 state [1], the $J = 1$ member of the D -wave spin-triplet charmonium states. Until now there have been no definitive observations of its two D -wave spin-triplet partner states, i.e., the 1^3D_2 and 1^3D_3 . Phenomenological models predict that the 1^3D_2 charmonium state has large decay widths to $\gamma\chi_{c1}$ and $\gamma\chi_{c2}$ [11]. In 1994, the E705 experiment reported a candidate for the 1^3D_2 state with a mass of 3836 ± 13 MeV/ c^2 and a statistical significance of 2.8σ [12]. Recently, the Belle Collaboration reported evidence for a narrow resonance $X(3823) \rightarrow \gamma\chi_{c1}$ in B meson decays with 3.8σ significance and mass $3823.1 \pm 1.8(\text{stat}) \pm 0.7(\text{syst})$ MeV/ c^2 , and suggested that this is a good candidate for the 1^3D_2 charmonium

state [13]. In the following, we denote the 1^3D_2 state as ψ_2 and the $\psi(3686)$ [$\psi(2S)$] state as ψ' .

In this Letter, we report a search for the production of the ψ_2 state via the process $e^+e^- \rightarrow \pi^+\pi^-X$, using 4.67 fb^{-1} data collected with the BESIII detector operating at the BEPCII storage ring [14] at center-of-mass (CM) energies that range from $\sqrt{s} = 4.19$ to 4.60 GeV [15]. The ψ_2 candidates are reconstructed in their $\gamma\chi_{c1}$ and $\gamma\chi_{c2}$ decay modes, with $\chi_{c1,c2} \rightarrow \gamma J/\psi$ and $J/\psi \rightarrow \ell^+\ell^-$ ($\ell = e$ or μ). A GEANT4-based [16] Monte Carlo (MC) simulation software package is used to optimize event selection criteria, determine the detection efficiency, and estimate the backgrounds. For the signal process, we generate 40,000 $e^+e^- \rightarrow \pi^+\pi^-X(3823)$ events at each CM energy indicated above, using an EVTGEN [17] phase space model, with $X(3823) \rightarrow \gamma\chi_{c1,c2}$. Initial state radiation (ISR) is simulated with KKMC [18], where the Born cross section of $e^+e^- \rightarrow \pi^+\pi^-X(3823)$ between 4.1 and 4.6 GeV is assumed to follow the $e^+e^- \rightarrow \pi^+\pi^-\psi'$ lineshape [19]. The maximum ISR photon energy is set to correspond to the 4.1 GeV/ c^2 production threshold of the $\pi^+\pi^-X(3823)$ system. Final-State-Radiation is handled with PHOTOS [20].

Events with four charged tracks with zero net charge are selected as described in Ref. [6]. Showers identified as photon candidates must satisfy fiducial and shower quality as well as timing requirements as described in Ref. [21]. At least two good photon candidates in each event are required. To improve the momentum and energy resolution and to reduce the background, the event is subjected to a four-constraint (4C) kinematic fit to the hypothesis $e^+e^- \rightarrow \pi^+\pi^-\gamma\gamma\ell^+\ell^-$, that constrains the total four-momentum of the detected particles to the initial four-momentum of the colliding beams. The χ^2 of the kinematic fit is required to be less than 80 (with an efficiency of about 95% for signal events). For multi-photon events, the two photons returning the smallest χ^2 from the 4C fit are assigned to be the radiative photons.

To reject radiative Bhabha and radiative dimuon ($\gamma e^+e^-/\gamma\mu^+\mu^-$) backgrounds associated with photon conversion, the cosine of the opening angle of the pion-pair candidates is required to be less than 0.98. This restric-

tion removes almost all Bhabha and dimuon background events, with an efficiency loss that is less than 1% for signal events. The background from $e^+e^- \rightarrow \eta J/\psi$ with $\eta \rightarrow \pi^+\pi^-\pi^0/\gamma\pi^+\pi^-$ is effectively rejected by the invariant mass requirement $M(\gamma\gamma\pi^+\pi^-) > 0.57 \text{ GeV}/c^2$. MC simulation shows that this requirement removes less than 1% of the signal events. In order to remove possible backgrounds from $e^+e^- \rightarrow \gamma_{\text{ISR}}\psi' \rightarrow \gamma_{\text{ISR}}\pi^+\pi^-J/\psi$, accompanied with a fake photon or a second ISR photon, $e^+e^- \rightarrow \eta\psi'$ with $\eta \rightarrow \gamma\gamma$, and $e^+e^- \rightarrow \gamma\gamma\psi'$, the invariant mass of $\pi^+\pi^-J/\psi$ is required to satisfy $|M(\pi^+\pi^-J/\psi) - m(\psi')| > 6 \text{ MeV}/c^2$ [22]. The signal efficiency for the ψ' mass window veto is 85% at $\sqrt{s} = 4.420 \text{ GeV}$ and $\geq 99\%$ at other energies.

After imposing the above requirements, there are clear J/ψ peaks in the $M(\ell^+\ell^-)$ invariant mass distributions for the data. The J/ψ mass window is defined as $3.08 < M(\ell^+\ell^-) < 3.13 \text{ GeV}/c^2$. The mass resolution is determined to be $9 \text{ MeV}/c^2$ by MC simulation. In order to evaluate non- J/ψ backgrounds, we define J/ψ mass sidebands as $3.01 < M(\ell^+\ell^-) < 3.06 \text{ GeV}/c^2$ or $3.15 < M(\ell^+\ell^-) < 3.20 \text{ GeV}/c^2$, which are twice as wide as the signal region. The combination of the higher energy photon (γ_H) with the J/ψ candidate is used to reconstruct $\chi_{c1,c2}$ signals, while the lower one is assumed to originate from the $X(3823)$ decay. We define the invariant mass range $3.490 < M(\gamma_H J/\psi) < 3.530 \text{ GeV}/c^2$ as the χ_{c1} signal region, and $3.536 < M(\gamma_H J/\psi) < 3.576 \text{ GeV}/c^2$ as the χ_{c2} signal region [$M(\gamma_H J/\psi) = M(\gamma_H \ell^+\ell^-) - M(\ell^+\ell^-) + m(J/\psi)$].

To investigate the possible existence of resonances that may decay to $\gamma\chi_{c1,c2}$, we examine two-dimensional scatter plots of $M_{\text{recoil}}(\pi^+\pi^-)$ versus $M(\gamma_H J/\psi)$. Here, $M_{\text{recoil}}(\pi^+\pi^-) = \sqrt{(P_{e^+e^-} - P_{\pi^+} - P_{\pi^-})^2}$ is the recoil mass of the $\pi^+\pi^-$ pair, where $P_{e^+e^-}$ and P_{π^\pm} are the 4-momenta of the initial e^+e^- system and the π^\pm , respectively. For this, we use the $\pi^+\pi^-$ momenta before the 4C fit correction because of the good resolution for low momentum pion tracks, as observed from MC simulation. Figure 1 shows $M_{\text{recoil}}(\pi^+\pi^-)$ versus $M(\gamma_H J/\psi)$ for data at different energies, where $e^+e^- \rightarrow \pi^+\pi^-\psi' \rightarrow \pi^+\pi^-\gamma\chi_{c1,c2}$ signals are evident in almost all data sets. In addition, event accumulations near $M_{\text{recoil}}(\pi^+\pi^-) \simeq 3.82 \text{ GeV}/c^2$ are evident in the χ_{c1} signal regions of the $\sqrt{s} = 4.36$ and 4.42 GeV data sets. A scatter plot of all the data sets combined is shown in Fig. 1 (f), where there is a distinct cluster of events near $3.82 \text{ GeV}/c^2$ (denoted hereafter as the $X(3823)$) in the χ_{c1} signal region.

The remaining backgrounds mainly come from $e^+e^- \rightarrow (\eta'/\gamma\omega)J/\psi$, with $(\eta'/\omega) \rightarrow \gamma\gamma\pi^+\pi^-/\gamma\pi^+\pi^-$, and $\pi^+\pi^-\pi^+\pi^-(\pi^0/\gamma\gamma)$. The $e^+e^- \rightarrow (\eta'/\gamma\omega)J/\psi$ backgrounds can be measured and simulated using the same data sets. The $e^+e^- \rightarrow \pi^+\pi^-\pi^+\pi^-(\pi^0/\gamma\gamma)$ mode can be evaluated with the J/ψ mass sideband data. All these backgrounds are found to be small, and they produce flat contributions to the $M_{\text{recoil}}(\pi^+\pi^-)$ mass distribution. There also might be $e^+e^- \rightarrow \pi^+\pi^-\psi'$ events with $\psi' \rightarrow \eta J/\psi$ and $\pi^0\pi^0 J/\psi$, but such kind of events would not affect the ψ' mass in the $M_{\text{recoil}}(\pi^+\pi^-)$ distribution.

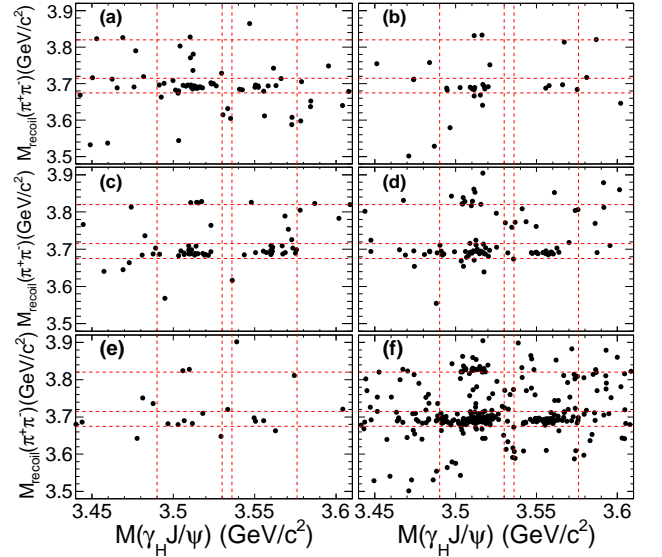


FIG. 1. Scatter plots of $M_{\text{recoil}}(\pi^+\pi^-)$ vs. $M(\gamma_H J/\psi)$ at (a) $\sqrt{s} = 4.230$, (b) 4.260 , (c) 4.360 , (d) 4.420 , and (e) 4.600 GeV . The sum of all the data sets is shown in (f). In each plot, the vertical dashed red lines represent χ_{c1} (left two lines) and χ_{c2} (right two lines) signal regions, and the horizontal lines represent the ψ' mass range (bottom two lines) and 3.82 GeV (top line), respectively.

An unbinned maximum likelihood fit to the $M_{\text{recoil}}(\pi^+\pi^-)$ invariant mass distribution is performed to extract the $X(3823)$ signal parameters. The signal shapes are represented by MC-simulated ψ' and $X(3823)$ (with input mass of $3.823 \text{ GeV}/c^2$ and a zero width) histograms, convolved with Gaussian functions with mean and width parameters left free in the fit to account for the mass and resolution difference between data and MC simulation, respectively. The background is parameterized as a linear function, as indicated by the J/ψ mass sideband data. The ψ' signal is used to calibrate the absolute mass scale and the resolution difference between data and simulation, which is expected to be similar for the $X(3823)$ and ψ' . A simultaneous fit with a common $X(3823)$ mass is applied to the data sets with independent signal yields at $\sqrt{s} = 4.230, 4.260, 4.360, 4.420$ and 4.600 GeV (data sets with small luminosities are merged to nearby data sets with larger luminosities), for the $\gamma\chi_{c1}$ and $\gamma\chi_{c2}$ modes, respectively.

Figure 2 shows the fit results, which return $M[X(3823)] = M[X(3823)]_{\text{input}} + \mu_{X(3823)} - \mu_{\psi'} = 3821.7 \pm 1.3 \text{ MeV}/c^2$ for the $\gamma\chi_{c1}$ mode, where $M[X(3823)]_{\text{input}}$ is the input $X(3823)$ mass in MC simulation, $\mu_{X(3823)} = 1.9 \pm 1.3 \text{ MeV}/c^2$ and $\mu_{\psi'} = 3.2 \pm 0.6 \text{ MeV}/c^2$ are the mass shift values for $X(3823)$ and ψ' histograms from the fit. The fit yields 19 ± 5 $X(3823)$ signal events in the $\gamma\chi_{c1}$ mode. The statistical significance of the $X(3823)$ signal in the $\gamma\chi_{c1}$ mode is estimated to be 6.2σ by comparing the difference between the log-likelihood value ($\Delta(\ln \mathcal{L}) = 27.5$) with or without $X(3823)$ signal in the fit, and taking the change of the number of degrees of freedom ($\Delta\text{ndf} = 6$) into account,

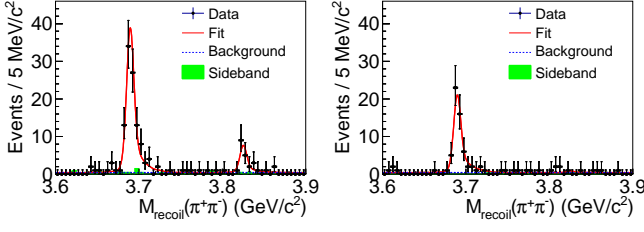


FIG. 2. Simultaneous fit to the $M_{\text{recoil}}(\pi^+\pi^-)$ distribution of $\gamma\chi_{c1}$ events (left) and $\gamma\chi_{c2}$ events (right), respectively. Dots with error bars are data, red solid curves are total fit, dashed blue curves are background, and the green shaded histograms are J/ψ mass sideband events.

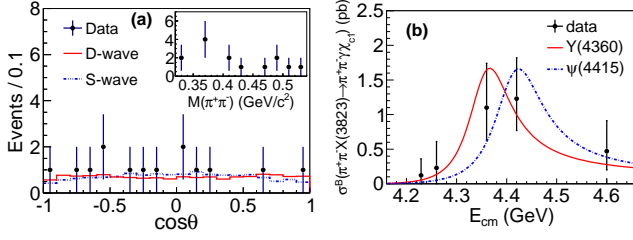


FIG. 3. (a) The $X(3823)$ scattering angle distribution for $X(3823)$ signal events, the inset shows the corresponding $M(\pi^+\pi^-)$ invariant mass distribution per $20 \text{ MeV}/c^2$ bin; and (b) fit to the energy-dependent cross section of $\sigma^B[e^+e^- \rightarrow \pi^+\pi^-X(3823)] \cdot \mathcal{B}(X(3823) \rightarrow \gamma\chi_{c1})$ with the $Y(4360)$ (red solid curve) and the $\psi(4415)$ (blue dashed curve) lineshapes. Dots with error bars are data. The red solid (blue dashed) histogram in (a) is MC simulation with D -wave (S -wave).

and its value is found to be larger than 5.9σ with various systematic checks. For the $\gamma\chi_{c2}$ mode, we do not observe an $X(3823)$ signal and provide an upper limit on its production rate (Table I). The limited statistics preclude a measurement of the intrinsic width of $X(3823)$. From a fit using a Breit-Wigner function (with a width parameter that is allowed to float) convolved with Gaussian resolution, we determine $\Gamma[X(3823)] < 16 \text{ MeV}$ at the 90% confidence level (C.L.) (including systematic errors).

The $X(3823)$ is a candidate for the ψ_2 charmonium state with $J^{PC} = 2^{--}$ [13]. In the $e^+e^- \rightarrow \pi^+\pi^-\psi_2$ process, the $\pi^+\pi^-$ system is very likely to be dominated by S -wave. Thus, a D -wave between the $\pi^+\pi^-$ system and ψ_2 is expected, with an angular distribution of $1 + \cos^2\theta$ for ψ_2 in the e^+e^- CM frame. Figure 3 (a) shows the angular distribution ($\cos\theta$) of $X(3823)$ signal events selected by requiring $3.82 < M_{\text{recoil}}(\pi^+\pi^-) < 3.83 \text{ GeV}/c^2$. The inset shows the corresponding $M(\pi^+\pi^-)$ invariant mass distribution per $20 \text{ MeV}/c^2$ bin. A Kolmogorov [23] test to the angular distribution gives the Kolmogorov statistic $D_{14,\text{obs}}^D = 0.217$ for the D -wave hypothesis and $D_{14,\text{obs}}^S = 0.182$ for the S -wave hypotheses. Due to limited statistics, both hypothesis can be accepted ($D_{14,\text{obs}}^D, D_{14,\text{obs}}^S < D_{14,0.1} = 0.314$) at the 90% C.L.

The product of the Born-order cross section and the branching ratio of $X(3823) \rightarrow \gamma\chi_{c1,c2}$ is calculated using $\sigma^B[e^+e^- \rightarrow \pi^+\pi^-X(3823)] \cdot \mathcal{B}[X(3823) \rightarrow \gamma\chi_{c1,c2}] = \frac{N_{c1,c2}^{\text{obs}}}{\mathcal{L}_{\text{int}}(1+\delta) \frac{1}{|1-\Pi|^2} \epsilon \mathcal{B}_{c1,c2}}$, where $N_{c1,c2}^{\text{obs}}$ is the number of $X(3823) \rightarrow \gamma\chi_{c1,c2}$ signal events obtained from a fit to the $M_{\text{recoil}}(\pi^+\pi^-)$ distribution, \mathcal{L}_{int} is the integrated luminosity, ϵ is the detection efficiency, $\mathcal{B}_{c1,c2}$ is the branching fraction of $\chi_{c1,c2} \rightarrow \gamma J/\psi \rightarrow \gamma \ell^+\ell^-$ and $(1 + \delta)$ is the radiative correction factor, which depends on the lineshape of $e^+e^- \rightarrow \pi^+\pi^-X(3823)$. Since we observe large cross sections at $\sqrt{s} = 4.360$ and 4.420 GeV , we assume the $e^+e^- \rightarrow \pi^+\pi^-X(3823)$ cross section follows that of $e^+e^- \rightarrow \pi^+\pi^-\psi'$ over the full energy range of interest and use the $e^+e^- \rightarrow \pi^+\pi^-\psi'$ lineshape from published results [19] as input in the calculation of the efficiency and radiative correction factor. The vacuum polarization factor $\frac{1}{|1-\Pi|^2}$ is calculated from QED with 0.5% uncertainty [24]. The results of these measurements for the data sets with large luminosities at $\sqrt{s} = 4.230, 4.260, 4.360, 4.420$ and 4.600 GeV are listed in Table I. Since at each single energy data the $X(3823)$ signal is not very significant, upper limits for production cross sections at the 90% C.L. based on the Bayesian method are given [systematic effects are included by convolving the $X(3823)$ signal events yield (n^{yield}) dependent likelihood curves with a Gaussian with mean value zero and standard deviation $n^{\text{yield}} \cdot \sigma_{\text{sys}}$, where σ_{sys} is the systematic uncertainty of the efficiencies]. The corresponding production ratio of $\mathcal{R}_{\psi'} = \frac{\sigma^B[e^+e^- \rightarrow \pi^+\pi^-X(3823)] \cdot \mathcal{B}[X(3823) \rightarrow \gamma\chi_{c1}]}{\sigma^B[e^+e^- \rightarrow \pi^+\pi^-\psi'] \cdot \mathcal{B}[\psi' \rightarrow \gamma\chi_{c1}]}$ is also calculated at $\sqrt{s} = 4.360$ and 4.420 GeV .

We fit the energy-dependent cross sections of $e^+e^- \rightarrow \pi^+\pi^-X(3823)$ with the $Y(4360)$ shape or the $\psi(4415)$ shape with their resonance parameters fixed to the PDG values [2]. Figure 3 (b) shows the fit results, which give $D_{5,\text{obs}}^{\text{H1}} = 0.151$ for the $Y(4360)$ hypothesis (H1) and $D_{5,\text{obs}}^{\text{H2}} = 0.169$ for the $\psi(4415)$ hypothesis (H2), based on the Kolmogorov test. Thus, we accept both the $Y(4360)$ and the $\psi(4415)$ hypotheses ($D_{5,\text{obs}}^{\text{H1}}, D_{5,\text{obs}}^{\text{H2}} < D_{5,0.1} = 0.509$) at the 90% C.L.

The systematic uncertainties in the $X(3823)$ mass measurement include those from the absolute mass scale, resolution, the parameterization of the $X(3823)$ signal, and the background shape. Since we use the ψ' signal to calibrate the fit, we conservatively take the uncertainty of $0.6 \text{ MeV}/c^2$ in the calibration procedure as the systematic uncertainty due to the mass scale. The resolution difference between the data and MC simulation is also estimated by the ψ' signal. Varying the resolution parameter by $\pm 1\sigma$, the mass difference in the fit is $0.2 \text{ MeV}/c^2$, which is taken as the systematic uncertainty from resolution. In the $X(3823)$ mass fit, a MC-simulated histogram with the width of $X(3823)$ set to zero is used to parameterize the signal shape. We replace this histogram with a simulated $X(3823)$ resonance with a width of 1.7 MeV [13] and repeat the fit; the change in the mass for this fit, $0.2 \text{ MeV}/c^2$, is taken as the systematic uncertainty due to the signal parameterization. Likewise, changes measured with a background shape from MC-simulated $(\eta'/\gamma\omega)J/\psi$

TABLE I. Number of observed events (N^{obs}), integrated luminosities (\mathcal{L}) [15], detection efficiency (ϵ) for the $X(3823) \rightarrow \gamma\chi_{c1}$ mode, radiative correction factor ($1 + \delta$), vacuum polarization factor ($\frac{1}{|1-\Pi|^2}$), measured Born cross section $\sigma^B(e^+e^- \rightarrow \pi^+\pi^-X(3823))$ times $\mathcal{B}_1(X(3823) \rightarrow \gamma\chi_{c1})$ ($\sigma_X^B \cdot \mathcal{B}_1$) and $\mathcal{B}_2(X(3823) \rightarrow \gamma\chi_{c2})$ ($\sigma_X^B \cdot \mathcal{B}_2$), and measured Born cross section $\sigma^B(e^+e^- \rightarrow \pi^+\pi^-\psi')$ ($\sigma_{\psi'}^B$) at different energies. Other data sets with lower luminosity are not listed. The numbers in the brackets correspond to the upper limit measurements at the 90% C.L. The relative ratio $\mathcal{R}_{\psi'} = \frac{\sigma^B[e^+e^- \rightarrow \pi^+\pi^-X(3823)]\mathcal{B}(X(3823) \rightarrow \gamma\chi_{c1})}{\sigma^B[e^+e^- \rightarrow \pi^+\pi^-\psi']\mathcal{B}(\psi' \rightarrow \gamma\chi_{c1})}$ is also calculated. The first errors are statistical, and the second systematic.

\sqrt{s} (GeV)	\mathcal{L} (pb $^{-1}$)	N^{obs}	ϵ	$1 + \delta$	$\frac{1}{ 1-\Pi ^2}$	$\sigma_X^B \cdot \mathcal{B}_1$ (pb)	$\sigma_X^B \cdot \mathcal{B}_2$ (pb)	$\sigma_{\psi'}^B$ (pb)	$\mathcal{R}_{\psi'}$
4.230	1092	$0.7^{+1.4}_{-0.7}$ (< 3.8)	0.168	0.755	1.056	$0.12^{+0.24}_{-0.12} \pm 0.02$ (< 0.64)	-	$34.1 \pm 8.1 \pm 4.7$	-
4.260	826	$1.1^{+1.8}_{-1.2}$ (< 4.6)	0.178	0.751	1.054	$0.23^{+0.38}_{-0.24} \pm 0.04$ (< 0.98)	-	$25.9 \pm 8.1 \pm 3.6$	-
4.360	540	$3.9^{+2.3}_{-1.7}$ (< 8.2)	0.196	0.795	1.051	$1.10^{+0.64}_{-0.47} \pm 0.15$ (< 2.27)	(< 1.92)	$58.6 \pm 14.2 \pm 8.1$	$0.20^{+0.13}_{-0.10}$
4.420	1074	$7.5^{+3.6}_{-2.8}$ (< 13.4)	0.145	0.967	1.053	$1.23^{+0.59}_{-0.46} \pm 0.17$ (< 2.19)	(< 0.54)	$33.4 \pm 7.8 \pm 4.6$	$0.39^{+0.21}_{-0.17}$
4.600	567	$1.9^{+1.8}_{-1.1}$ (< 5.4)	0.157	1.075	1.055	$0.47^{+0.44}_{-0.27} \pm 0.07$ (< 1.32)	-	$10.4^{+6.4}_{-4.7} \pm 1.5$	-

events or a second-order polynomial indicate a systematic uncertainty associated with the background shape of 0.2 MeV/ c^2 in mass. Assuming that all the sources are independent, the total systematic uncertainty is calculated by adding the individual uncertainties in quadrature, resulting in 0.7 MeV/ c^2 for the $X(3823)$ mass measurement. For the $X(3823)$ width, we measure the upper limits with the above systematic checks, and report the most conservative one.

The systematic uncertainties in the cross section measurement mainly come from efficiencies, signal parameterization, background shape, decay model, radiative correction, and luminosity measurement. The luminosity is measured using Bhabha events, with an uncertainty of 1.0%. The uncertainty in the tracking efficiency for high momenta leptons is 1.0% per track. Pions have momenta that range from 0.1 to 0.6 GeV/ c , and the momentum-weighted uncertainty is 1.0% per track. In this analysis, the radiative transition photons have energies from 0.3 to 0.5 GeV. Studies with a sample of $J/\psi \rightarrow \rho\pi$ events show that the uncertainty in the reconstruction efficiency for photons in this energy range is less than 1.0%.

The same sources of signal parameterization and background shape as discussed in the systematic uncertainty of $X(3823)$ mass measurement would contribute 4.0% and 8.8% differences in $X(3823)$ signal events yields, which are taken as systematic uncertainties in the cross section measurement. Since the $X(3823)$ is a candidate for the ψ_2 charmonium state, we try to model the $e^+e^- \rightarrow \pi^+\pi^-X(3823)$ process with a D -wave in the MC simulation. The efficiency difference between D -wave model and three-body phase space is 3.8%, which is quoted as the systematic uncertainty for the decay model. The $e^+e^- \rightarrow \pi^+\pi^-X(3823)$ lineshape affects the radiative correction factor and detection efficiency. The radiator function is calculated from QED with 0.5% precision [25]. As discussed above, both $Y(4360)$ lineshapes [19, 26] and the $\psi(4415)$ lineshape describe the cross section of $e^+e^- \rightarrow \pi^+\pi^-X(3823)$ reasonably well. We take the difference for $(1 + \delta) \cdot \epsilon$ between $Y(4360)$ lineshapes and the $\psi(4415)$ lineshape as its systematic uncertainty, which is 6.5%.

Since the event topology in this analysis is quite similar

to $e^+e^- \rightarrow \gamma\pi^+\pi^-J/\psi$ [10], we use the same systematic uncertainties for the kinematic fit (1.5%) and the J/ψ mass window (1.6%). The uncertainties on the branching ratios for $\chi_{c1,c2} \rightarrow \gamma J/\psi$ (3.6%) and $J/\psi \rightarrow \ell^+\ell^-$ (0.6%) are taken from the PDG [2]. The uncertainty from MC statistics is 0.3%. The efficiencies for other selection criteria, the trigger simulation [27], the event-start-time determination, and the final-state-radiation simulation are very high (> 99%), and their systematic uncertainties are estimated to be less than 1%.

Assuming that all the systematic uncertainty sources are independent, we add all of them in quadrature. The total systematic uncertainty in the cross section measurements is estimated to be 13.8%.

In summary, we observe a narrow resonance, $X(3823)$, through the process $e^+e^- \rightarrow \pi^+\pi^-X(3823)$ with a statistical significance of 6.2σ . The measured mass of the $X(3823)$ is $(3821.7 \pm 1.3 \pm 0.7)$ MeV/ c^2 , where the first error is statistical and the second systematic, and the width is less than 16 MeV at the 90% C.L. Our measurement agrees well with the values found by Belle [13]. The production cross sections of $\sigma^B(e^+e^- \rightarrow \pi^+\pi^-X(3823)) \cdot \mathcal{B}(X(3823) \rightarrow \gamma\chi_{c1}, \gamma\chi_{c2})$ are also measured at $\sqrt{s} = 4.230, 4.260, 4.360, 4.420,$ and 4.600 GeV.

The $X(3823)$ resonance is a good candidate for the $\psi(1^3D_2)$ charmonium state. According to potential models [1], the D -wave charmonium states are expected to be within a mass range of 3.82 to 3.85 GeV. Among these, the $1^1D_2 \rightarrow \gamma\chi_{c1}$ transition is forbidden due to C-parity conservation, and the amplitude for $1^3D_3 \rightarrow \gamma\chi_{c1}$ is expected to be small [28]. The mass of $\psi(1^3D_2)$ is in the 3.810 \sim 3.840 GeV/ c^2 range that is expected for several phenomenological calculations [29]. In this case, the mass of $\psi(1^3D_2)$ is above the $D\bar{D}$ threshold but below the $D\bar{D}^*$ threshold. Since $\psi(1^3D_2) \rightarrow D\bar{D}$ violates parity, the $\psi(1^3D_2)$ is expected to be narrow, in agreement with our observation, and $\psi(1^3D_2) \rightarrow \gamma\chi_{c1}$ is expected to be a dominant decay mode [29, 30]. From our cross section measurement, the ratio $\frac{\mathcal{B}[X(3823) \rightarrow \gamma\chi_{c2}]}{\mathcal{B}[X(3823) \rightarrow \gamma\chi_{c1}]} < 0.42$ (where systematic uncertainties cancel) at the 90% C.L. is obtained, which also agrees with expectations for the $\psi(1^3D_2)$ state [30].

The BESIII collaboration thanks the staff of BEPCII and the IHEP computing center for their strong support. This work is supported in part by National Key Basic Research Program of China under Contract No. 2015CB856700; National Natural Science Foundation of China (NSFC) under Contracts Nos. 11125525, 11235011, 11322544, 11335008, 11425524; the Chinese Academy of Sciences (CAS) Large-Scale Scientific Facility Program; the CAS Center for Excellence in Particle Physics (CCEPP); Joint Large-Scale Scientific Facility Funds of the NSFC and CAS under Contracts Nos. 11179007, U1232201, U1332201; CAS under Contracts Nos. KJCX2-YW-N29, KJCX2-YW-N45; 100 Talents Program of CAS; INPAC and Shanghai Key Laboratory for Particle Physics and Cosmology; German Research Founda-

tion DFG under Contract No. Collaborative Research Center CRC-1044; Seventh Framework Programme of the European Union under Marie Curie International Incoming Fellowship Grant Agreement No. 627240; Istituto Nazionale di Fisica Nucleare, Italy; Ministry of Development of Turkey under Contract No. DPT2006K-120470; Russian Foundation for Basic Research under Contract No. 14-07-91152; U.S. Department of Energy under Contracts Nos. DE-FG02-04ER41291, DE-FG02-05ER41374, DE-FG02-94ER40823, DESC0010118; U.S. National Science Foundation; University of Groningen (RuG) and the Helmholtzzentrum fuer Schwerionenforschung GmbH (GSI), Darmstadt; WCU Program of National Research Foundation of Korea under Contract No. R32-2008-000-10155-0.

-
- [1] E. Eichten, K. Gottfried, T. Kinoshita, K. D. Lane, and T. M. Yan, *Phys. Rev. D* **17**, 3090 (1978); *Phys. Rev. D* **21**, 203 (1980).
- [2] K. A. Olive *et al.* (Particle Data Group), *Chin. Phys. C* **38**, 090001 (2014).
- [3] S. K. Choi *et al.* (Belle Collaboration), *Phys. Rev. Lett.* **91**, 262001 (2003).
- [4] B. Aubert *et al.* (BaBar Collaboration), *Phys. Rev. Lett.* **95**, 142001 (2005).
- [5] Z. Q. Liu *et al.* (Belle Collaboration), *Phys. Rev. Lett.* **110**, 252002 (2013).
- [6] M. Ablikim *et al.* (BESIII Collaboration), *Phys. Rev. Lett.* **110**, 252001 (2013).
- [7] T. Xiao, S. Dobbs, A. Tomaradze and K. K. Seth, *Phys. Lett. B* **727**, 366 (2013).
- [8] N. Brambilla *et al.*, *Eur. Phys. J. C* **71**, 1534 (2011).
- [9] Eric Swanson, *Physics* **6**, 69 (2013).
- [10] M. Ablikim *et al.* (BESIII Collaboration), *Phys. Rev. Lett.* **112**, 092001 (2014).
- [11] E. J. Eichten, K. Lane, and C. Quigg, *Phys. Rev. Lett.* **89**, 162002 (2002); P. Cho and M. B. Wise, *Phys. Rev. D* **51**, 3352 (1995).
- [12] L. Antoniazzi *et al.* (The E705 Collaboration), *Phys. Rev. D* **50**, 4258 (1994).
- [13] V. Bhardwaj *et al.* (Belle Collaboration), *Phys. Rev. Lett.* **111**, 032001 (2013).
- [14] M. Ablikim *et al.* (BESIII Collaboration), *Nucl. Instrum. Methods Phys. Res., Sect. A* **614**, 345 (2010).
- [15] M. Ablikim *et al.* (BESIII Collaboration), arXiv:1503.03408 [hep-ex] (2015).
- [16] S. Agostinelli *et al.* (GEANT4 Collaboration), *Nucl. Instrum. Methods A* **506**, 250 (2003).
- [17] D. J. Lange, *Nucl. Instrum. Methods A* **462**, 152 (2001).
- [18] S. Jadach, B. F. L. Ward, and Z. Was, *Comput. Phys. Commun.* **130**, 260 (2000); *Phys. Rev. D* **63**, 113009 (2001).
- [19] X. L. Wang *et al.* (Belle Collaboration), arXiv:1410.7641.
- [20] P. Golonka, and Z. Was, *Eur. Phys. J. C* **45**, 97 (2006).
- [21] M. Ablikim *et al.* (BESIII Collaboration), *Phys. Rev. D* **86**, 071101(R) (2012).
- [22] In this Letter, $M(\pi^+\pi^-J/\psi) = M(\pi^+\pi^-\ell^+\ell^-) - M(\ell^+\ell^-) + m(J/\psi)$ is used to partly cancel the mass resolution of the lepton pair. Here $m(J/\psi)$ and $m(\psi')$ are the nominal masses of J/ψ and ψ' [2].
- [23] A. Kolmogorov, *G. Inst. Ital. Attuari.* **4**, 83 (1933).
- [24] F. Jegerlehner, *Z. Phys. C* **32** (1986) 195.
- [25] E. A. Kuraev and V. S. Fadin, *Yad. Fiz.* **41**, 733 (1985) [*Sov. J. Nucl. Phys.* **41**, 466 (1985)].
- [26] J. P. Lees *et al.* (BaBar Collaboration), *Phys. Rev. D* **89**, 111103 (R) (2014).
- [27] N. Berger *et al.*, *Chin. Phys. C*, **34** (12), 1779-1784 (2010).
- [28] T. Barnes, S. Godfrey and E. S. Swanson, *Phys. Rev. D* **72**, 054026 (2005).
- [29] S. Godfrey and N. Isgur, *Phys. Rev. D* **32**, 189 (1985); W. Kwong, J. Rosner, and C. Quigg, *Annu. Rev. Nucl. Part. Phys.* **37**, 343 (1987); D. Ebert, R. N. Faustov, and V. O. Galkin, *Phys. Rev. D* **67**, 014027 (2003); E. J. Eichten, K. Lane, and C. Quigg, *Phys. Rev. D* **69**, 094019 (2004); M. Blank and A. Krassnigg, *Phys. Rev. D* **84**, 096014 (2011).
- [30] C. F. Qiao, F. Yuan, and K. T. Chao, *Phys. Rev. D* **55**, 4001 (1997).